Reconstructed centennial variability of Late Holocene storminess from Cors Fochno, Wales, UK

Orme, L. C. ; Davies, S. J.; Duller, G. A. T.

Published in:
Journal of Quaternary Science

DOI:
10.1002/jqs.2792

Publication date:
2015

Citation for published version (APA):
Orme, L. C., Davies, S. J., & Duller, G. A. T. (2015). Reconstructed centennial variability of Late Holocene storminess from Cors Fochno, Wales, UK. *Journal of Quaternary Science*, *30*(5), 478-488. https://doi.org/10.1002/jqs.2792

Published in Journal of Quaternary Science 2015, volume 30. DOI: 10.1002/jqs.2792

Reconstructed centennial variability of Late Holocene storminess from Cors Fochno, Wales, UK

Orme, L.C.[1, 2] (lco203@exeter.ac.uk), Davies, S.J.[1], Duller, G.A.T.[1]

[1] Department of Geography and Earth Sciences, Aberystwyth University, Llandinam Building, Penglais Campus, Aberystwyth, Wales, SY23 3DB UK

[2] Geography Department, University of Exeter, Amory Building, Streatham Campus, Exeter, EX4 4QJ UK

Abstract

Future anthropogenic climate forcing is forecast to increase storm intensity and frequency over Northern Europe, due to a northward shift of the storm tracks, and a positive North Atlantic Oscillation (NAO). However understanding the significance of such a change is difficult since the natural variability of storminess beyond the range of instrumental data is poorly known. Here we present a decadal resolution record of storminess covering the Late Holocene, based on a 4 m long core taken from the peat bog of Cors Fochno in mid-Wales, UK. Storminess is indicated by variations in the minerogenic content as well as bromine deposited from sea spray. Twelve episodes of enhanced storm activity are identified during the last 4.5 cal ka BP. Although the age model gives some uncertainty in the timings, it appears that storminess increased at the onset and close of North Atlantic cold events associated with oceanic changes, with reduced storm activity at their peak. Cors Fochno is strongly influenced by westerly moving storms, so it is suggested that the patterns were due to variations in the intensity of westerly airflow and atmospheric circulation during times when the latitudinal temperature gradient was steepened.

Keywords: storminess, Holocene, North Atlantic Oscillation, UK, storm track

Introduction

The most intense and damaging storms affecting Europe originate in the Atlantic and impact upon the western seaboard. During the period December 2013 to February 2014 the United Kingdom was affected by frequent, intense storms that caused extensive flooding and infrastructural damage (Kendon and McCarthy, 2015). These storms were caused by a number of factors, including a persistent southward perturbation of the jet stream over North America and a strong polar vortex (Slingo *et al*., 2014). Similar winter conditions are forecasted in response to global warming; predictions suggest that over the next century the storm track will shift northwards and storm frequency will increase in the British Isles, due to an intensified jet stream (Pinto *et al*., 2009; Stocker *et al*., 2013). However making such predictions is problematic, as there is poor understanding of natural variability and relatively short instrumental storminess records (Allan *et al*., 2009; von Storch and Weisse, 2008). Thus there is a requirement for continuous and high resolution reconstructions spanning the Late Holocene that capture changes in the frequency and intensity of storms, termed 'storminess'. The western coast of Wales is a key location for reconstructing these past changes, as recent storms demonstrate that intensification of the jet stream leads to enhanced storminess in this region (Slingo *et al.,* 2014).

The North Atlantic Oscillation (NAO) is a measure of the pressure difference between the Azores High pressure and the Icelandic Low pressure (Hurrell, 1995). A greater pressure difference during positive NAO anomalies results in the storm track crossing northern Europe and an increased storm intensity, while negative NAO anomalies (with reduced pressure gradients) cause the storm track to cross southern Europe (Hurrell, 1995). During the instrumental period, the NAO is a dominant control on storminess in Europe particularly during the winter months (Allan *et al*., 2009), however research has shown a more complex relationship between storminess and the NAO during the Late Holocene (Dawson *et al*., 2002; Trouet *et al*., 2012). The Little Ice Age (LIA, c. 0.55-0.15 cal ka BP; 1400-1800 C.E.) is thought to have had more negative NAO conditions (e.g. Trouet *et al*., 2009, 2012). However records indicate storminess was high *across* Europe during this time, rather than only in southern Europe as would typically be expected from negative NAO conditions (e.g. Sorrel *et al*., 2012). It has been hypothesised that during the LIA a

steepened temperature gradient caused high intensity but low frequency storms (Lamb, 1995), consistent with a dominant negative NAO (Trouet *et al*., 2012).

The causes of centennial scale storminess variability through the Late Holocene are debated, with oceanic and solar forcings frequently suggested. Reconstructions of oceanic circulation from the North Atlantic region have shown LIA-type events occur with a periodicity of c.1470 ± 500 years; polar waters spread to more southern latitudes, with a weaker Atlantic Meridional Overturning Circulation, North Atlantic Current and subpolar gyre (Bianchi and McCave, 1999; Bond *et al*., 1997; Thornalley *et al*., 2009). These episodes have been linked with increased storminess in Europe and southward storm track shifts, suggested as being the result of cold ocean temperatures at high latitudes causing a steepened temperature gradient (Sorrel *et al*., 2012; Fletcher *et al*., 2012; Sabatier *et al*., 2012). However other studies have emphasised the importance of solar minima as a main or additional cause of high storminess (Martin-Puertas *et al*., 2012; Sabatier *et al*., 2012; Mellström *et al*., 2015). Further storm reconstructions from Europe are needed to improve the spatial and temporal understanding of storminess. For example, opposite patterns between northern and southern Europe could indicate storm track shifts associated with NAO variability. Furthermore, improved understanding should help to untangle the key drivers of storminess in northwest Europe and their relationship to Late Holocene cold events.

A number of methods have been used to obtain extended records of storminess proxies. In Greenland, sea-source sodium concentrations in ice cores provide a proxy of sea-spray (Meeker and Mayewski, 2002). In Europe the deposition of coastal dunes are a proxy for increased wind strength and hence storminess (Clarke *et al*., 2002; Clarke and Rendell, 2006; Clemmensen *et al*., 2009). Other methods include over-wash deposits in coastal lagoons (Sabatier *et al*., 2012), cliff-top storm deposits (CTSDs) left by extreme waves (e.g. Hansom and Hall, 2009) and marine records reflecting wind-blown current strength and storm deposits (e.g. Andresen *et al*., 2005; Billeaud *et al*., 2009; Hass, 1996; Sorrel *et al*., 2009). However, all of these methods have potential problems. Dunes are prone to reworking, which bias the record towards more recent events, and it is not clear whether the date of deposition of coastal dunes records the period of most intense aeolian flux, or the waning stage of a period of enhanced activity. Other records such as CTSDs and sand layers

within coastal lagoons show only the most extreme events, with erosion potentially causing a bias towards recent events (Haslett and Bryant, 2007), although preservation is good at some sites (Dezileau *et al*., 2011; Sabatier *et al.,* 2008).

The aeolian flux of minerogenic material onto peat bogs can be used as a more direct measure of wind strength and hence storminess. Björck and Clemmensen (2004) counted the number of minerogenic grains above 0.2 mm diameter delivered to the surface of two bogs in southwest Sweden per unit time. They termed this the Aeolian Sand Influx (ASI) and although the method of analysis was extremely labour-intensive they preferred ASI to a simple measure of the inorganic residue because their bogs also contained significant silt sized minerogenic component from far-travelled dust. The same approach has subsequently been applied to a number of sites in Europe (e.g. De Jong *et al*., 2006, 2009; Sjögren, 2009) and in South America (Björck *et al.,* 2012). Reconstructions using this method are often high resolution and continuous, however natural or human alterations to the landscapes surrounding the bogs may influence the amount of sand deposition at times, so must be considered in the interpretation of these records.

This study targets a unique site located in the extreme west of the United Kingdom, which provides an ideal location to apply the aeolian flux methods pioneered by Björck and Clemmensen (2004). The key to this approach is the juxtaposition of a westerly facing seashore, with an abundant supply of sand sized material that can be deflated, in close proximity to a continuously aggrading ombrotrophic bog, which can act as a trap for the minerogenic material. The main aim of this study is to produce a high resolution record of storminess for the western margin of the United Kingdom through the Late Holocene using the influx of aeolian sand as a proxy. A secondary aim is to test the effectiveness of bromine (Br) measurements from micro X-ray fluorescence (μXRF) core scanning as an indicator of storminess. As a marine aerosol, Br records have been interpreted as representing past storm activity (e.g. Unkel *et al*., 2010; Turner *et al*., 2014; Schofield *et al.,* 2010). However, Br is also known to accumulate in organic matter and be influenced by humification (e.g. Biester *et al.,* 2004). Comparison of Br profiles with independent records of storminess is needed to validate the potential of this technique. As rapid, high-resolution datasets can be obtained with μXRF-scanning

(Croudace *et al*., 2006), it is potentially a valuable addition to the range of methods available for reconstructing past storm activity from peat bog deposits.

Study Area

Cors Fochno is a 650 ha ombrotrophic raised peat bog situated in Cardigan Bay, mid-Wales, lying to the east of the 3-4 km long Borth Beach and Ynyslas sand dunes, which act as a sediment source during storms (Figure 1). Station measurements (1981-2010 A.D.) from Llanbedr, located on the coast 30 km north of Cors Fochno, show an annual mean wind speed of 9.4 knots (0.51 m s^{-1}) (Met Office, 2015). The bog is composed predominantly of sphagnum peat and has developed over a mid-Holocene forest bed since c. 4.7 cal ka BP (Shi and Lamb, 1991; Wilks, 1979), with the central dome reaching a thickness of 5 m (Hughes and Schulz, 2001). The bog is situated to the south of the village of Borth, The margins have been modified by peat cutting in recent centuries and an artificial channel has been created for the Afon Leri; however the central dome is unaffected by these changes and it forms the largest area of primary raised bog in lowland Britain (Poucher, 2009). The ecological importance and unique oceanic setting of the bog have contributed to its Ramsar status and its inclusion in the UNESCO Dyfi Biosphere. Palaeoenvironmental research has previously been carried out on Cors Fochno to investigate local pollution, vegetation change and coastal and sea level changes (Hughes and Schulz, 2001; Mighall *et al*., 2009; Moore, 1968).

Methods

Two cores were taken from Cors Fochno using a Russian corer: a short core (*core 1*) from the northern edge of the bog at 52º30’28”N, 4º1’17”W, and a main long core (*core 2*) from a central site at 52º30’9”N, 4º0’39”W (Figure 1). Cores were wrapped securely in the field and subsequently stored at 4°C. Core 1 was to a depth of 1 m, although the active peat in the acrotelm (upper 18 cm) was not preserved during coring so has not been analysed. At the central site, a 4 m sequence was obtained; again the acrotelm (upper 14 cm) was not preserved during coring.

Cores were subsampled into u-channels to ensure a consistent sample surface and scanned using an ITRAX µXRF core scanner at a resolution of 200 µm (30kV, 30mA, 12 second count). The µXRF bromine (Br) results were normalised using the incoherent + coherent peaks, which represent Compton and Rayleigh scattering and provide an estimation of the organic and water content of the sediments.

The sediment within the u-channels was then sliced into 1 cm sections, so that known sample volumes were used (each 2.3 cm^3). Loss-on-ignition was used to separate the minerogenic material from the peat. Samples were dried at 105ºC overnight, ignited in a furnace at 550ºC for 4 hours and weighed between every stage (Dean, 1974; Heiri *et al*., 2001). This allowed the Ignition Residue (IR) to be calculated, which was the ignited weight as a percentage of the dried weight, and shows the quantity of inorganic material in the sample. This also allowed the Organic Bulk Density (OBD) of each sample to be calculated, which can be a measure of peat humification (Björck and Clemmensen, 2004):

OBD ($g\ cm^{-3}$) = (dried weight - ignited weight) / sample volume

To assess the relationship between the IR measurement and sand content within the peat, we determined the Aeolian Sand Influx (ASI) over two sections using the approach of Björck and Clemmensen (2004). The IR samples collected from depths of 14-110 cm and 150-200 cm in Core 2 were treated twice with 10% hydrochloric acid to remove any carbonates, then with 30% hydrogen peroxide to remove any remnant organics that may have survived ignition, before being mounted on glycerine jelly slides and analysed under a microscope. The number of grains with a diameter over 200 µm was counted, and the diameter of the largest grain in each sample was recorded. We used the same lower threshold for counting grains as the original research by Björck and Clemmensen (2004). The ASI was then calculated:

ASI = (number of grains > 200µm / sample volume) / number of years in 1 cm of peat

The age-depth model for the main core (core 2) was developed from AMS radiocarbon dates from five bulk peat samples. The calibration and age model was constructed using Bayesian analysis by OxCal version 4.2.2, which used the Intcal13

calibration curve (Ramsey, 2009; Reimer *et al*., 2013). Spectral analysis was carried out on the IR results using a normalised Lomb-Scargle fourier transform (Shoelson, 2001), which is a method of spectral analysis that can identify frequency signals in unevenly spaced data (Lomb, 1976; Press and Rybicki, 1989; Scargle, 1982).

Results

The cores consist of dark brown sphagnum peat throughout, but with variations in the degree of humification, as shown by the OBD results (Figure 2). Below 2 m depth there is dense, humified peat while above 2 m there are greater variations in the density and degree of humification.

The results from the five radiocarbon dates are shown in Table 1, including the median probability of the 2 σ range and the errors representing the analytical error propagated through the calibration software. The 4 m core spans the last 4.5 cal ka BP. The upper radiocarbon date at 50 cm depth had a modern age, thought to be due to contamination, so this age was not included in the age-depth model. The four other ages and known age of the modern bog surface at 0 cm depth were used to create the age-depth model (Figure 2). This shows a consistent peat accumulation rate of ~0.8-1.2 mm/year, similar to the rate of growth calculated by Hughes and Schulz (2001) for the bog during the period from 7.04 to 3.27 ^{14}C ka BP. Mighall *et al*. (2009) obtained a chronology for a peat core from the centre of Cors Fochno covering the period from 3.63 ^{14}C ka BP to the present day. The ^{210}Pb dates for the upper 17 cm, and a series of radiocarbon dates from 53 cm to 325 cm depth, confirmed an essentially constant accumulation rate at this site, and is very similar to our age model. The lack of age-control in our study between 130 cm depth and the surface means that there is additional chronological uncertainty in this interval for our core, but comparison with these others studies implies that any discrepancies should be small.

The comparison between the ASI, IR and maximum grain sizes over two sections showed that there was less similarity between the ASI and IR results with depth. Maximum grain size also decreased downcore (Figure 3). In the main core (core 2) the average IR is 2.2%, and throughout much of the core the IR results vary

from this by less than 1% (Figure 4), However, in some parts of the core there are higher IR values, reaching a maximum of 6.8%, with some peaks spanning depths of >10 cm. The IR results revealed twelve peaks at: 4.46-4.44, 3.98-3.92, 3.77-3.61, 3-2.97, 2.84-2.8, 2.31-2.24, 2.09-1.97, 1.56-1.55, 1.4-1.35, 1.09-1.05, 0.58-0.47 and 0.21-0.12 cal ka BP (Figure 4). The bromine record shows peaks at c. 3.9, 3.4, 3.3, 2.9, 2.8, 2.3, 1.9, 1.7, 1.4, 0.9, 0.5 and 0.2 cal ka BP. The Lomb-Scargle spectral analysis shows the Cors Fochno IR record has cycles that are significant at the 95% confidence limit with periodicities of 1740, 870, 445, 395, 315 and 290 years (Figure 5).

Proxy Interpretation

By comparing the ASI, IR and maximum grain size results in two sections (Figure 3) it was clear that with depth in the core the ASI no longer captured changes in sand content due to smaller grain sizes. Sites in Scandinavia where the ASI method has been used have a significant fine dust input originating from long distance transport of grains (Björck and Clemmensen, 2004), so it was necessary for the ASI proxy to be used to measure the coarse sand and exclude the fine sand and silt fractions, which may not have been indicative of storms. Cors Fochno however can be expected to have had minimal fine dust input because it is on the Atlantic seaboard, meaning the IR results here give an unambiguous storminess signal. The IR is a preferable proxy because the ASI relies on correctly defining the minimum threshold for counting grains. It is suggested that a gradual sea level rise during the Mid-Late Holocene at this site resulted in a transgression (Kidson and Heyworth, 1978); the change in distance between the coring site and the beach appears to have altered the size of sand grain reaching the core site over time (Figure 3). Therefore at Cors Fochno the use of the IR was considered the most appropriate proxy for detecting storminess when considering the location, environmental evolution of the surrounding area and the limitations of the ASI method.

Archaeological evidence suggests a human presence in the area throughout the Late Holocene but particularly since the early 19th century, when there was land drainage and diversion of the River Leri, greater agriculture, the building of a railway track and expansion of Borth (Poucher, 2009). It is noteworthy that many of the

archaeological sites are situated to the east and south-east of Cors Fochno, so the prevailing westerly winds would not transport sediment onto the bog from these. As the beach and dunes are in close proximity to the bog and in the path of the prevailing winds, we consider that these have been the dominant source of sand delivered to Cors Fochno, with the human activities resulting in a negligible level of disturbance prior to the 19th century.

The similarity between the independent IR and Br records suggest that both are capturing storminess signals rather than human activity as Br (a marine aerosol) is less likely to be affected by anthropogenic disturbance. The position of the site on the western seaboard of Wales mean that these most likely represent periods of increased westerly storm activity. However there is a discrepancy between the two proxies at 3.7 cal ka BP, with very high IR values but low Br. This may have been caused by local factors, such as human disturbance, though there is no independent evidence for this. Alternatively, as Br will be more easily transported than sand, the concentrations in the bog may reflect storm frequency rather than intensity, so this may have been a time of generally low storminess punctuated with a number of intense storms capable of sand transport. Phases of enhanced storminess (shown by the sand influx) last for between 10 and 160 years. The peaks have an average age error of ±160 years but with greater uncertainty before 3.8 cal ka BP and after 1.34 cal ka BP.

Discussion

European Spatial Patterns of Storminess

Records of storminess from Europe have been compiled to show temporal as well as spatial changes over the Late Holocene (Figure 6). Analysing multiple reconstructions within a region reduces the impact of local factors and methodological limitations. Comparing sites from northern and southern Europe may also allow changes related to storm track shifts and the NAO to be detected.

During the last 2000 years the Cors Fochno reconstruction (Figure 6F) shows four peaks in storminess which, despite large age errors in both reconstructions, appear to be in phase with strengthened bottom water currents in the Skagerrak

Sea, thought to be driven by westerly storms (Hass, 1996; Figure 6G). Storm reconstructions from around northern Europe, including Scotland and Northern Ireland as well as Scandinavia and France, show some but not all of these events (see references within Figure 6). Together the results support that the Cors Fochno storminess record is capturing a regional climate signal, and that northern and central Europe have experienced greater storminess at c. 1.5, 1.05, 0.5 and 0.1 cal ka BP. A similar comparison of European reconstructions by Sorrel *et al*. (2012) suggested that during the last 2000 years storminess was higher across Europe at 1.9-1.05 and 0.6-0.25 cal ka BP. Our comparison agrees with these broad periods but indicates that within these times storminess was more variable, with periods of increased storminess lasting around 100-200 years.

In southern Europe the identification of storm events during the last 2000 years is less certain as a result of fewer available reconstructions. In Portugal, sand dune development at 1.5 and 0.1 cal ka BP (Clarke and Rendell, 2006; Figure 6M) occurs at similar times to the periods of high storminess seen in northern Europe, so may indicate increases in storminess across mainland Europe. Similarly a Mediterranean storm reconstruction, measuring wave overtopping of a lagoon barrier, shows high storminess during the periods 1.95-1.4 and 0.4-0.05 cal ka BP (Sabatier *et al*., 2012; Figure 6N), although these are longer periods of increased storm activity than those identified in northern Europe.

The reconstructions from the high latitudes (Figure 6 A-C) show conflicting patterns of storminess. A proxy for bottom current strength on the Icelandic shelf indicates that storminess increased between 1.1-0.7 cal ka BP (Andresen *et al*., 2005, Figure 6B). However a terrestrial proxy of loess grainsize in Iceland suggests increased storminess between c.2-1 cal ka BP and to a lesser degree after 0.5 cal ka BP (Jackson *et al*., 2005, Figure 6C), while the GISP2 sea spray proxy supports the finding that there was increased storminess after 0.5 cal ka BP (Mayewski *et al*., 1997; Figure 6A).

The Cors Fochno record suggests that the period between 4.5 and 2 cal ka BP had as frequent storms as the time since 2 cal ka BP. The large peak in the Cors Fochno reconstruction at c.3.7 cal ka BP is not clearly shown in the other reconstructions, however the enhanced storminess between around 2.3-2 cal ka BP

is in agreement with a single reconstruction in Scandinavia and another from Portugal (Figure 6 I and M). There are also indications that storminess increased widely in Europe c. 2.9 cal ka BP, with peaks in Wales, Scandinavia, France, Ireland and Greenland at this time (Figure 6; Mellström *et al.,* 2015), as well as in coastal deposits in northwest Spain (Gonzalez-Ãlvarez *et al*., 2005).

The compiled storm reconstructions indicate that during the last 2000 years periods of enhanced storminess were simultaneous (within dating error) across northern Europe, during the LIA (0.55 and 0.1 cal ka BP) and around 1.1 and 1.5 cal ka BP. The pattern is less clear before 2 cal ka BP, most likely due to fewer records, although there is some suggestion that widespread storminess increases occurred c.2.9 cal ka BP and there was potentially a period of enhanced storminess at 3.7 cal ka BP.

Storm Track Shifts

The LIA appears to have had high storminess particularly over the transitions (c.0.6-0.4 and c.0.2-0.05 cal ka BP) from the Medieval Climate Anomaly and post-AD 1900, although the uncertainty in the age of the peak at 0.6-0.4 cal ka BP is 200 years. Nevertheless fluvial flooding reconstructions from northern, western and central Europe, also show increases at 0.7-0.4 and 0.2-0.05 cal ka BP (Rumsby and Macklin, 1996). Between these periods, during the mid-LIA, reconstructions have contradictory findings for the magnitude of storminess. Some indicate intense storms in northern Europe at this time (Lamb, 1995; Wheeler *et al*., 2010) and in spring and autumn a more southerly storm track is believed to have crossed the British Isles (Luterbacher *et al*., 2001). However the Cors Fochno reconstruction suggests reduced storminess during the mid-LIA and there is thought to have been reduced flooding in northern and central Europe (Rumsby and Macklin, 1996). Furthermore a proxy reconstruction of wind-driven Atlantic Water Inflow into the Norwegian Sea suggests that the storm track was not in a northerly position during the LIA (Giraudeau *et al*., 2010). This reduced storminess in the Cors Fochno reconstruction may in part result from the bogs location making it sensitive to westerly tracking storms. Westerly airflow was suggested as the cause of the increased flooding at the LIA transitions (Rumsby and Macklin, 1996), while at the peak of the LIA (the

Maunder Minimum, 1645-1715 A.D.) documentary and modelling evidence has indicated that there were more meridional circulation patterns, blocking high pressures across northern Europe, a southerly storm track in winter and lower precipitation particularly on Britain's west coast (Jacobeit *et al.,* 2003; Lamb, 1966; Luterbacher *et al*., 2001; Raible *et al*., 2007). In support of this, reconstructions from across southern Europe suggest precipitation and flooding increased between 0.45-0.25/0.15 cal ka BP (Benito *et al*., 1996; Magny *et al*., 2008; Pfister, 1984). Therefore these findings support the idea that storminess increased during the LIA, potentially due to a steepened temperature gradient (Trouet *et al*., 2012), however they also support that circulation patterns and storm track shifts were important.

A similar pattern can be observed during the period 1.55-1.05 cal ka BP. As during the LIA, temperatures in the extra-tropical northern hemisphere were lower between c.1.65-1.15 cal ka BP, during what is often termed the Dark Ages cold period (Ljungqvist, 2010). The reconstructions presented imply that northern Europe experienced increased storminess at c.1.56-1.35 and c.1.09-1.05 cal ka BP, and this is supported by documentary evidence pieced together by Lamb (1995), showing increased storminess c.1.4 and 1.1 cal ka BP. In the intervening period, as during the LIA, southerly storm tracks are indicated by the north-south index based on Norwegian glacier reconstructions, with a maximum southerly extent at 1.2 cal ka BP (Bakke *et al*., 2008), and by reconstructions suggesting increased precipitation and flooding in southern Europe at this time (Arnaud *et al*., 2005; Magny *et al*., 2007). However as the wind-driven Atlantic water inflow into the Norwegian Sea remained fairly high (Giraudeau *et al*., 2010), it is possible that the storm track shift was not as persistent or as far south as during the LIA.

Oceanic and Atmospheric Circulation Changes

During the instrumental period the NAO is the dominant control on storminess. We compare the Cors Fochno storm reconstruction with an NAO reconstruction based on weather-driven changes in hypolimnic anoxia from a lake from south west Greenland (Olsen *et al*., 2012; Figure 7E). This indicates that storm events coincide with some negative NAO periods, particularly since 2.2 cal ka BP (c.1.1, 1.4, 1.6 and 2.1 cal ka BP), however the earlier section of the record before 2.2 cal ka BP does

not show increased storminess at times of negative NAO. As the locations of the NAO pressure centres are non-stationary (Schmutz *et al*., 2000), it is possible that the NAO influence on regional climate has changed over the Late Holocene, which may explain the lower correspondence in the earlier part of the record. As hypothesised for the LIA (Trouet *et al.,* 2012) a steepened temperature gradient may have caused intensified storms despite frequent negative NAO patterns at the times of high storminess since 2.2 cal ka BP. These may have been climate transitions associated with both high, westerly storminess in northern Europe as well as negative NAO conditions. Although contradictory, as weather patterns vary on the timescales of days-weeks it is likely that periods with frequent negative NAO anomalies could also have had strong westerly airflow across northern Europe. Overall the cold events of the Late Holocene may have had a steepened meridional temperature gradient, like the LIA, which resulted in periods characterised by both strengthened westerly airflow as well as NAO negative events.

Oceanic forcing of storminess is suggested by the dominant cycle of 1740 years in the Cors Fochno record. Similar length cycles have been found in other reconstructions of cyclonic activity (precipitation and wind) from the Mediterranean, Iceland and Greenland (Debret *et al.,* 2007; Fletcher *et al*., 2013; Giraudeau *et al.,* 2000; Jackson *et al.,* 2005; O'Brien *et al.,* 1995). It has been suggested that the 1700 year cycle is the result of internal oceanic forcing, which imprints on cyclonic activity in the North Atlantic, as the 1700 year cycle has been identified in North Atlantic marine cores (Bianchi and McCave, 1999; Debret *et al*., 2007; Fletcher *et al*., 2013; Giraudeau *et al*., 2000).

This ocean-atmosphere relationship is potentially supported by comparing the Cors Fochno storminess reconstruction with those reflecting the strength of the N. Atlantic thermohaline circulation (Figure 7 and references therein), although dating errors in parts of our reconstruction and the marine reconstructions make such comparisons difficult. There appear to be increases in storminess at the transitions of periods with weak thermohaline circulation, as shown by high ice-rafting debris (IRD) concentrations in North Atlantic cores (showing when polar waters moved south; Figure 7B), and reduced strength of the Iceland-Scotland Overflow Water (ISOW; Figure 7C) and sub-polar gyre (SPG) circulation (Figure 7D). These changes occurred during the above described LIA (c.0.6-0.05 cal ka BP) and Dark Ages

412 (c.1.6-1.05 cal ka BP), although the SPG strength proxy shows some difference in
413 the timing of the weakening during the Dark Ages. Earlier in the Late Holocene the
414 ISOW speed was reduced between 4.2-3.5 and 3-2.2 cal ka BP, the SPG circulation
415 weakened c.4.5-3.8 and 3-2 cal ka BP and the IRD increased at c.4 cal ka BP
416 (Figure 7 B-D). At the transitions of these periods the Cors Fochno period has single
417 or pairs of periods with enhanced storm activity (Figure 7A), although the increases
418 in the IRD at c.2.8 cal ka BP occur simultaneously with high storminess in records
419 from Europe. The Cors Fochno reconstruction indicates that at the transitions of LIA-
420 type events during the Late Holocene storminess (or westerly airflow) may have
421 increased in northern Europe.

422 Solar maxima and minima have both been suggested as causes of variations in
423 storminess (Gleisner and Thejll, 2003; Huth *et al*., 2006; Lamb, 1991; Mayewski *et*
424 *al*., 2005; Poore *et al*., 2003; Wheeler *et al*., 2010; Mellström *et al.,* 2015). This may
425 be supported by cycles of 445 and 320 years in the Cors Fochno record, which are
426 similar to 420 and 315 year solar cycles (Stuiver and Braziunas, 1989; Poore *et al*.,
427 2003), although the centennial-length cycles may have been distorted by the age
428 errors. The comparison between the Cors Fochno reconstruction and the total solar
429 irradiance (TSI) reconstruction (Figure 7F; Steinhilber *et al*., 2008) does not indicate
430 that storminess increased at either solar maxima or minima, therefore it is not
431 possible to ascertain a solar influence on storminess.

432

433

434

435

436

437

438

439

440

Conclusion

Aeolian-transport of sand onto the coastal ombrotrophic peat bog of Cors Fochno, situated on the west coast of Wales, has allowed a storminess reconstruction to be made spanning 4500 years. Twelve peaks in storminess have been identified at 4.46-4.44, 3.98-3.92, 3.77-3.61, 3-2.97, 2.84-2.8, 2.31-2.24, 2.09-1.97, 1.56-1.55, 1.4-1.35, 1.09-1.05, 0.58-0.47 and 0.21-0.12 cal ka BP. Comparison between sand content and normalised μXRF bromine measurements support the use of bromine as a proxy for sea spray and therefore storminess in peat bogs.

By comparison with other European Late Holocene storminess reconstructions it is possible to identify synchronous increases in storminess across northern Europe. The Cors Fochno reconstruction and others in northern Europe show enhanced storminess at the transitions of times that were calm and cold, at 1.6-1 cal ka BP and 0.55-0.05 cal ka BP (LIA). Evidence indicates that the ocean circulation in the North Atlantic during these periods, and similar events of the Late Holocene, was weakened, and the identified storm events occur at the transitions of these times. The 1740 year cycle found in the Cors Fochno reconstruction has also been found in westerly wind and oceanic proxies elsewhere also suggesting a link with oceanic variability. The findings support the hypothesis that a steeper temperature gradient increased storm intensity across Europe during the LIA (Trouet *et al*., 2012; Lamb, 1995) and similar events earlier in the Late Holocene; however these times were temporally variable, possibly as the result of circulation variability and episodes of strengthened westerly airflow.

Acknowledgments

This research benefitted from the Climate Change Consortium for Wales (C3W). Financial support was provided by Aberystwyth University (for radiocarbon dating). We would like to thank Natural Resources Wales and Mike Bailey for granting access to the site as well as providing fieldwork assistance. We are also grateful to Henry Lamb, Rachel Smedley and Hannah Bailey for fieldwork assistance. We thank James Scourse and two anonymous reviewers for their constructive comments.

Bibliography

Allan R, Tett S, Alexander L. 2009. Fluctuations in autumn–winter severe storms over the British Isles: 1920 to present. *International Journal of Climatology* **29**: 357-371.

Andresen CS, Bond G, Kuijpers A, Knutz PC, Björck S. 2005. Holocene climate variability at multidecadal time scales detected by sedimentological indicators in a shelf core NW off Iceland. *Marine Geology* **214**: 323-338.

Arnaud F, Revel M, Chapron E, Desmet M, Tribovillard N. 2005. 7200 years of Rhône river flooding activity in Lake Le Bourget, France: a high-resolution sediment record of NW Alps hydrology. *The Holocene* **15**: 420-428.

Bakke J, Lie Ø, Dahl SO, Nesje A, Bjune AE. 2008. Strength and spatial patterns of the Holocene wintertime westerlies in the NE Atlantic region. *Global and Planetary Change* **60**: 28-41.

Benito G, Machado MJ, Pérez-González A. 1996. Climate change and flood sensitivity in Spain. *Geological Society, London, Special Publications* **115**: 85-98.

Bianchi G, McCave IN. 1999. Holocene periodicity in North Atlantic climate and deep-ocean flow south of Iceland. *Nature* **397**: 515-517.

Biester H, Keppler F, Putschew A, Martínez-Cortizas A, Petri M. 2004, Halogen retention, organohalogens, and the role of organic matter decomposition on halogen enrichment in two Chilean peat bog. *Environmental Science & Technology* **38**: 1984-1991.

Billeaud I, Tessier B, Lesueur P. 2009. Impacts of late Holocene rapid climate changes as recorded in a macrotidal coastal setting (Mont-Saint-Michel Bay, France). *Geology* **37**: 1031-1034.

Björck S, Clemmensen LB. 2004. Aeolian sediment in raised bog deposits, Halland, SW Sweden: a new proxy record of Holocene winter storminess variation in Southern Scandinavia? *The Holocene* **14**: 677-688.

Björck S, Rundgren M, Ljung K, Unkel I, Wallin ÃS. 2012. Multi-proxy analyses of a peat bog on Isla de los Estados, easternmost Tierra del Fuego: a unique record of

501 the variable Southern Hemisphere Westerlies since the last deglaciation. *Quaternary*
502 *Science Reviews* **42**: 1-14.

503 Bond G, Kromer B, Beer J, Muscheler R, Evans MN, Showers W, Hoffmann S, Lotti-
504 Bond R, Hajdas I, Bonani G. 2001. Persistent solar influence on North Atlantic
505 climate during the Holocene. *Science* **294**: 2130-2136.

506 Bond G, Showers W, Cheseby M, Lotti R, Almasi P, deMenocal P, Priore P, Cullen
507 H, Hajdas I, Bonani G. 1997. A pervasive millennial-scale cycle in North Atlantic
508 Holocene and glacial climates. *Science* **278**: 1257-1266.

509 Clarke M, Rendell H, Tastet J-P, Clave B, Masse L. 2002. Late-Holocene sand
510 invasion and North Atlantic storminess along the Aquitaine Coast, southwest France.
511 *The Holocene* **12**: 231-238.

512 Clarke M, Rendell HM. 2006. Effects of storminess, sand supply and the North
513 Atlantic Oscillation on sand invasion and coastal dune accretion in western Portugal.
514 *The Holocene* **16**: 341-355.

515 Clemmensen LB, Murray A, Heinemeier J, de Jong R. 2009. The evolution of
516 Holocene coastal dunefields, Jutland, Denmark: A record of climate change over the
517 past 5000 years. *Geomorphology* **105**: 303-313.

518 Croudace IW, Rindby A, Rothwell RG. 2006. ITRAX: description and evaluation of a
519 new multi-function X-ray core scanner. *Geological Society, London, Special*
520 *Publications* **267**: 51-63.

521 Dawson AG, Hickey K, Holt T, Elliott L, Dawson S, Foster IDL, Wadhams P,
522 Jonsdottir I, Wilkinson J, McKenna J, Davis NR, Smith DE. 2002. Complex North
523 Atlantic Oscillation (NAO) Index signal of historic North Atlantic storm-track changes.
524 *The Holocene* **12**: 363-369.

525 De Jong R, Björck S, Björkman L, Clemmensen LB. 2006. Storminess variation
526 during the last 6500 years as reconstructed from an ombrotrophic peat bog in
527 Halland, southwest Sweden. *Journal of Quaternary Science* **21**: 905-919.

De Jong R, Hammarlund D, Nesje A. 2009. Late Holocene effective precipitation variations in the maritime regions of south-west Scandinavia. *Quaternary Science Reviews* **28**: 54-64.

Dean WE. 1974. Determination of carbonate and organic matter in calcareous sediments and sedimentary rocks by loss on ignition; comparison with other methods. *Journal of Sedimentary Research* **44**: 242-248.

Debret M, Bout-Roumazeilles V, Grousset F, Desmet M, McManus J, Massei N, Sebag D, Petit J-R, Copard Y, Trentesaux A. 2007. The origin of the 1500-year climate cycles in Holocene North Atlantic records. *Climate of the Past* **3**: 679-692.

Dezileau L, Sabatier P, Blanchemanche P, Joly B, Swingedouw D, Cassou C, Castaings J, Martinez P, Von Grafenstein U. 2011. Intense storm activity during the Little Ice Age on the French Mediterranean coast. *Palaeogeography, Palaeoclimatology, Palaeoecology* **299**: 289-297.

Fletcher WJ, Debret M, Goni MFS. 2012. Mid-Holocene emergence of a low-frequency millennial oscillation in western Mediterranean climate: Implications for past dynamics of the North Atlantic atmospheric westerlies. *The Holocene* **23**: 153-166.

Giraudeau J, Cremer M, Manthé, S., Labeyrie, L., and Bond, G., 2000, Coccolith evidence for instabilities in surface circulation south of Iceland during Holocene times. *Earth and Planetary Science Letters* **179**: 257-268.

Giraudeau J, Grelaud M, Solignac S, Andrews JT, Moros M, Jansen E. 2010. Millennial-scale variability in Atlantic water advection to the Nordic Seas derived from Holocene coccolith concentration records. *Quaternary Science Reviews* **29**: 1276-1287.

Gleisner H, Thejll P. 2003. Patterns of tropospheric response to solar variability: *Geophysical Research Letters* **30**.

González-Ãlvarez, R., Bernárdez, P., Pena, L.D., Francés, G., Prego, R., Diz, P., and Vilas, F., 2005, Paleoclimatic evolution of the Galician continental shelf (NW of Spain) during the last 3000 years: from a storm regime to present conditions. *Journal of Marine Systems* **54**: 245-260.

Hansom JD, Hall AM. 2009. Magnitude and frequency of extra-tropical North Atlantic cyclones: A chronology from cliff-top storm deposits. *Quaternary International* **195**: 42-52.

Haslett SK, Bryant EA. 2007. Reconnaissance of historic (post-AD 1000) high-energy deposits along the Atlantic coasts of southwest Britain, Ireland and Brittany, France. *Marine Geology* **242**: 207-220.

Hass HC. 1996. Northern Europe climate variations during late Holocene: evidence from marine Skagerrak. *Palaeogeography, Palaeoclimatology, Palaeoecology* **123**: 121-145.

Heiri O, Lotter AF, Lemcke G. 2001. Loss on ignition as a method for estimating organic and carbonate content in sediments: reproducibility and comparability of results. *Journal of Paleolimnology* **25**: 101-110.

Hughes PDM, Schulz J. 2001. The development of the Borth Bog (Cors Fochno) mine system and the submerged forest beds at Ynyslas. In *The Quaternary of West Wales: Field Guide,* Walker M, McCarroll D (eds). Quaternary Research Association: London; 104-112.

Hurrell JW. 1995. Decadal Trends in the North-Atlantic Oscillation - Regional Temperatures and Precipitation. *Science* **269**: 676-679.

Hurrell JW, Deser C. 2010. North Atlantic climate variability: The role of the North Atlantic Oscillation. *Journal of Marine Systems* **79**: 231-244.

Huth R, Pokorná L, Bochníček J, Hejda P. 2006. Solar cycle effects on modes of low-frequency circulation variability. *Journal of Geophysical Research: Atmospheres* **111**: D22107.

Jackson MG, Oskarsson N, Trønnes RG, McManus JF, Oppo DW, Grönvold K, Hart SR, Sachs JP. 2005. Holocene loess deposition in Iceland: Evidence for millennial-scale atmosphere-ocean coupling in the North Atlantic. *Geology* **33**: 509-512.Jacobeit J, Wanner H, Luterbacher J, Beck C, Philipp A, Sturm K. 2003. Atmospheric circulation variability in the North-Atlantic-European area since the mid-seventeenth century. *Climate Dynamics* **20**: 341-352.

587 Kendon M, McCarthy M. 2015. The UK's wet and stormy winter of 2013/2014.
588 *Weather* **70**: 40-47.

589 Kidson C, Heyworth A. 1978. Holocene eustatic sea level change. *Nature* **273**: 748-
590 750.

591 Lamb F. 1991. *Historic Storms of the North Sea, British Isles and Northwest Europe*.
592 Cambridge University Press: Great Britain.

593 Lamb H. 1966. *The Changing Climate*. Methuen and co.: London.

594 Lamb H. 1995. *Climate, History and the Modern World*. Routledge: London.

595 Ljungqvist FC. 2010. A new reconstruction of temperature variability in the extra-
596 tropical Northern Hemisphere during the last two millennia. *Geografiska Annaler:*
597 *Series A, Physical Geography* **92**: 339-351.

598 Lomb NR. 1976. Least-squares frequency analysis of unequally spaced data.
599 *Astrophysics and space science* **39**: 447-462.

600 Luterbacher J, Rickli R, Xoplaki E, Tinguely C, Beck C, Pfister C, Wanner H. 2001.
601 The Late Maunder Minimum (1675-1715) - A Key Period for Studying Decadal Scale
602 Climatic Change in Europe. *Climatic Change* **49**: 441-462.

603 Magny M, de Beaulieu J-L, Drescher-Schneider R, Vannière B, Walter-Simonnet A-
604 V, Miras Y, Millet L, Bossuet G, Peyron O, Brugiapaglia E, Leroux A. 2007. Holocene
605 climate changes in the central Mediterranean as recorded by lake-level fluctuations
606 at Lake Accesa (Tuscany, Italy). *Quaternary Science Reviews* **26**: 1736-1758.

607 Magny M, Gauthier E, Vannière B, Peyron O. 2008. Palaeohydrological changes and
608 human-impact history over the last millennium recorded at Lake Joux in the Jura
609 Mountains, Switzerland. *The Holocene* **18**: 255-265.

610 Martin-Puertas C, Matthes K, Brauer A, Muscheler R, Hansen F, Petrick C, Aldahan
611 A, Possnert G, van Geel B. 2012. Regional atmospheric circulation shifts induced by
612 a grand solar minimum. *Nature Geosci*ence **5**: 397-401.

613 Mayewski PA, Meeker LD, Twickler MS, Whitlow S, Yang Q, Lyons WB, Prentice M.
614 1997. Major features and forcing of high-latitude northern hemisphere atmospheric

615 circulation using a 110,000-year-long glaciochemical series. *Journal of Geophysical*
616 *Research: Oceans (1978-2012)* **102**: 26345-26366.

617 Mayewski PA, Maasch KA, Yan Y, Kang S, Meyerson EA, Sneed SB, Kaspari SD,
618 Dixon DA, Osterberg EC, Morgan V. 2005. Solar forcing of the polar atmosphere.
619 *Annals of Glaciology* **41**: 147-154.

620 Meeker LD, Mayewski PA. 2002. A 1400-year high-resolution record of atmospheric
621 circulation over the North Atlantic and Asia. *The Holocene* **12**: 257-266.

622 Mellström A, Van Der Putten N, Muscheler R, De Jong R, Björck S. 2015. A shift
623 towards wetter and windier conditions in southern Sweden around the prominent
624 solar minimum 2750 cal a BP. *Journal of Quaternary Science* **30**: 235-244.

625 Met Office. 2015. Llanbedr station data.
626 http://www.metoffice.gov.uk/public/weather/climate/gcmh6hkcz [18 April 2015]

627 Mighall TM, Timberlake S, Foster IDL, Krupp E, Singh S. 2009. Ancient copper and
628 lead pollution records from a raised bog complex in Central Wales, UK. *Journal of*
629 *Archaeological Science* **36**: 1504-1515.

630 Moore P. 1968. Human influence upon vegetational history in North Cardiganshire.
631 *Nature* **217**: 1006-1009.

632 O'Brien SR, Mayewski PA, Meeker LD, Meese DA, Twickler MS, Whitlow SI. 1995.
633 Complexity of Holocene Climate as Reconstructed from a Greenland Ice Core.
634 *Science* **270**: 1962-1964.

635 Olsen J, Anderson NJ, Knudsen MF. 2012. Variability of the North Atlantic Oscillation
636 over the past 5,200 years. *Nature Geoscience* **5**: 808-812.

637 Pfister C. 1984. *Das Klima der Schweiz 1525-1860*, Academica Helvetica.Pinto JG,
638 Zacharias S, Fink AH, Leckebusch GC, Ulbrich U. 2009. Factors contributing to the
639 development of extreme North Atlantic cyclones and their relationship with the NAO.
640 *Climate Dynamics* **32**: 711-737.

641 Poore R, Dowsett H, Verardo S, Quinn TM. 2003. Millennial- to century- scale
642 variability in Gulf of Mexico Holocene climate records. P*aleoceanography* **18**.

643 Poucher P. 2009. *Wetland margins survey: Cors Fochno*. Dyfed Archaeological
644 Trust.

645 Press WH, Rybicki GB. 1989. Fast algorithm for spectral analysis of unevenly
646 sampled data. *The Astrophysical Journal* **338**: 277-280.

647 Raible C, Yoshimori M, Stocker T, Casty C. 2007. Extreme midlatitude cyclones and
648 their implications for precipitation and wind speed extremes in simulations of the
649 Maunder Minimum versus present day conditions. *Climate Dynamics* **28**: 409-423.

650 Ramsey CB. 2009. Bayesian analysis of radiocarbon dates. *Radiocarbon* **51**: 337-
651 360.

652 Reimer PJ, Bard E, Bayliss A, Beck JW, Blackwell PG, Ramsey CB, Buck CE,
653 Cheng H, Edwards RL, Friedrich M. 2013. IntCal13 and Marine13 radiocarbon age
654 calibration curves 0-50,000 years cal BP. *Radiocarbon* **55**: 1869-1887.

655 Rumsby BT, Macklin MG. 1996. River response to the last neoglacial (the “Little Ice
656 Age”) in northern, western and central Europe. *Geological Society, London, Special*
657 *Publications* **115**: 217-233.

658 Sabatier P, Dezileau L, Condomines M, Briqueu L, Colin C, Bouchette FR, Le Duff
659 M, Blanchemanche P. 2008. Reconstruction of paleostorm events in a coastal
660 lagoon (Hérault, South of France). *Marine Geology* **251**: 224-232.

661 Sabatier P, Dezileau L, Colin C, Briqueu L, Bouchette FDR, Martinez P, Siani G,
662 Raynal O, Von Grafenstein U. 2012. 7000 years of paleostorm activity in the NW
663 Mediterranean Sea in response to Holocene climate events. *Quaternary Research*
664 **77**: 1-11.

665 Scargle JD. 1982. Studies in astronomical time series analysis. II-Statistical aspects
666 of spectral analysis of unevenly spaced data. *The Astrophysical Journal* **263**: 835-
667 853.

668 Schmutz C, Luterbacher J, Gyalistras D, Xoplaki E, Wanner H. 2000. Can we trust
669 proxy-based NAO index reconstructions? *Geophysical Research Letters* **27**: 1135-
670 1138.

671 Schofield JE, Edwards KJ, Mighall TM, Martínez Cortizas A, Rodríguez-Racedo J,
672 Cook G. 2010. An integrated geochemical and palynological study of human
673 impacts, soil erosion and storminess from southern Greenland since c. AD 1000.
674 *Palaeogeography, Palaeoclimatology, Palaeoecology* **295**: 19-30.

675 Shi Z, Lamb HF. 1991. Post-glacial sedimentary evolution of a microtidal estuary,
676 Dyfi Estuary, west Wales, U.K. *Sedimentary Geology* **73**: 227-246.

677 Shoelson, B. (2001). http://www.mathworks.co.uk/matlabcentral/fileexchange/993-
678 lombscargle-m [6 July 2014]

679 Sjögren P. 2009. Sand mass accumulation rate as a proxy for wind regimes in the
680 SW Barents Sea during the past 3 ka. *The Holocene* **19**: 591-598.

681 Slingo J, Belcher S, Scaife A, McCarthy M, Saulter A, McBeath K, Jenkins A,
682 Huntingford C, Marsh T, Hannaford J. 2014. The recent storms and floods in the UK.
683 *Met Office Report.*

684 Sorrel P, Tessier B, Demory F, Delsinne N, Mouazé D. 2009. Evidence for millennial-
685 scale climatic events in the sedimentary infilling of a macrotidal estuarine system, the
686 Seine estuary (NW France). *Quaternary Science Reviews* **28**: 499-516.

687 Sorrel P, Debret M, Billeaud I, Jaccard S, McManus J, Tessier B. 2012. Persistent
688 non-solar forcing of Holocene storm dynamics in coastal sedimentary archives.
689 *Nature Geoscience* **5**: 892-896.

690 Steinhilber F, Abreu J, Beer J. 2008. Solar modulation during the Holocene.
691 *Astrophysics and Space Sciences Transactions* **4**: 1-6.

692 Steinhilber F, Beer J, Fröhlich C. 2009. Total solar irradiance during the Holocene.
693 *Geophysical Research Letters* **36**: L19704.

694 Stocker TF, Qin D, Plattner G-K, Tignor M, Allen SK, Boschung J, Nauels A, Xia Y,
695 Bex V, Midgley PM. 2013. *Climate change 2013: The physical science basis:*
696 *Intergovernmental Panel on Climate Change, Working Group I Contribution to the*
697 *IPCC Fifth Assessment Report (AR5)*: Cambridge University Press, New York.

698 Stuiver M, Braziunas TF. 1989. Atmospheric ^{14}C and century-scale solar oscillations.
699 *Nature* **338**: 405-408.

700 Thornalley DJ, Elderfield H, McCave IN. 2009. Holocene oscillations in temperature
701 and salinity of the surface subpolar North Atlantic. *Nature* **457**: 711-714.

702 Trouet V, Esper J, Graham NE, Baker A, Scourse JD, Frank DC. 2009. Persistent
703 positive North Atlantic Oscillation mode dominated the Medieval Climate Anomaly.
704 *Science*, **324**: 78-80.

705 Trouet V, Scourse JD, Raible CC. 2012. North Atlantic storminess and Atlantic
706 Meridional Overturning Circulation during the last Millennium: Reconciling
707 contradictory proxy records of NAO variability. *Global and Planetary Change* **84-85**:
708 48-55.

709 Turner TE, Swindles GT, Roucoux KH. 2014. Late Holocene ecohydrological and
710 carbon dynamics of a UK raised bog: impact of human activity and climate change.
711 *Quaternary Science Reviews*, **84**: 65-85.

712 Unkel I, Fernandez M, Björck S, Ljung K, Wohlfarth B. 2010. Records of
713 environmental changes during the Holocene from Isla de los Estados (54.4°S),
714 southeastern Tierra del Fuego. *Global and Planetary Change* **74**: 99-113.

715 von Storch H, Weisse R. 2008. Regional storm climate and related marine hazards
716 in the Northeast Atlantic. *Climate extremes and society*: 54-73.

717 Wheeler D, Garcia-Herrera R, Wilkinson CW, Ward C. 2010. Atmospheric circulation
718 and storminess derived from Royal Navy logbooks: 1685 to 1750. *Climatic Change*
719 **101**: 257-280.

720 Wilks P. 1979. Mid-Holocene sea-level and sedimentation interactions in the Dovey
721 estuary area, Wales. *Palaeogeography, Palaeoclimatology, Palaeoecology* **26**: 17-
722 36.

723 Wilson P, McGourty J, Bateman MD. 2004. Mid-to late-Holocene coastal dune event
724 stratigraphy for the north coast of Northern Ireland. *The Holocene* **14**: 406-416.

725

726

727

728 Table 1: Radiocarbon dates and calibrated ages from core 2, Cors Fochno.

Sample Depth (cm)	Laboratory Code	$\delta^{13}C$ (‰)	Radiocarbon Age (^{14}C yr BP ± 1σ)	Calibrated Age (2σ interval)	Calibrated Median age (cal yrs BP)
50-51	Beta-289917	-27.2	post-bomb	NA	NA
130-131	Beta-281364	-22.4	1700 ± 40	1705 - 1535	1610
185-186	Beta-289918	-25.6	2060 ± 30	2119 - 1946	2030
260-261	Beta-289919	-26.8	2760 ± 30	2941 - 2779	2850
330-331	Beta-281365	-26.2	3430 ± 40	3828 - 3586	3690

729

730

731

Figure Captions:

Figure 1: *left:* Location of Cors Fochno in the United Kingdom (inset) and map of the Dyfi estuary and Cors Fochno bog with the two coring locations. *Right:* Map of Europe showing the approximate locations of the NAO pressure centres (Hurrell and Deser, 2010) and sites of storminess reconstructions discussed in this research (letters corresponding to those in Figure 6).

Figure 2: *from left*: core 1 ignition residue results and core 2 ignition residue results, organic bulk density and age-depth model.

Figure 3: Comparison of the proxies for sand content in core 2: The Aeolian Sediment Influx, ignition residue and maximum grain size.

Figure 4: OBD, IR and Br/inc + coh results for core 2. Arrows highlight periods of enhanced storm activity shown by the IR and bromine proxies. The grey line on the bromine plot gives the raw measurements (0.2 mm resolution) and the black line the smoothed measurements (using a 1 cm moving average).

Figure 5: Lomb-Scargle Powerspectrum analysis of the IR results of core 2

Figure 6: Latitudinal differences of European storminess records
Sites (from top): **A** Greenland (Meeker and Mayewski, 2002), **B** Iceland (basalt/plagioclase ratio) (Andresen *et al*., 2005), **C** Iceland (Jackson *et al*., 2005), **D** Scotland (Hansom and Hall, 2009), **E** northern Ireland (Wilson *et al*., 2004) **F** Cors Fochno, Wales (*this study*) **G** Skagerrak Sea (Hass, 1996), **H** Halland Coast, Sweden (De Jong *et al*., 2006), **I** Denmark (Clemmensen *et al*., 2009), **J** Seine Estuary, France (Sorrel *et al*., 2009), **K** Mont-Saint-Michel Bay, France (Billeaud *et al*., 2009) **L** Aquitaine coast, France (Clarke *et al*., 2002), **M** Portugal (Clarke and Rendell, 2006) **N** French Mediterranean coast (Sabatier *et al*., 2012), Dotted lines show periods of enhanced storminess identified in the Cors Fochno reconstruction.

Figure 7: Comparison between the Cors Fochno storm reconstruction and potential forcings. From top: A) Cors Fochno storm reconstruction (*this study*), B) percentage of Haematite Stained Grains (HSG) from 4-stacked records from the North Atlantic as a proxy for IRD (Bond *et al*., 2001), C) mean sortable silt (10-63μm) mean size as a proxy for Iceland-Scotland Overflow Water (ISOW) current strength (Bianchi and

McCave, 1999), D) inferred water column stratification (density difference) based on temperature and salinity reconstructions from two planktonic foraminifera (*Globigerina bulloides* and *Globorotalia inflata*), which can be used as a proxy for Sub-Polar Gyre strength (Thornalley *et al*., 2009), E) reconstruction of the North Atlantic Oscillation index (Olsen *et al*., 2012), F) reconstructed Total Solar Irradiance (TSI) (Steinhilber *et al*., 2009). The dashed rectangles highlight the periods discussed in the text that appear to have weaker ocean circulation and peaks in storminess at the transitions."

Figure 1:

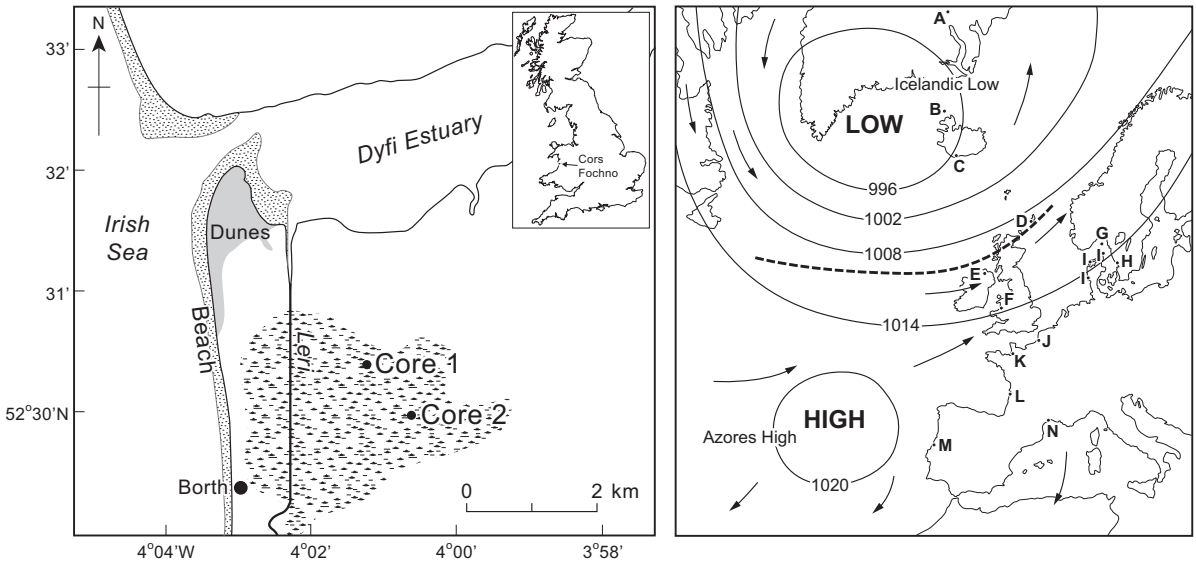

Figure 2:

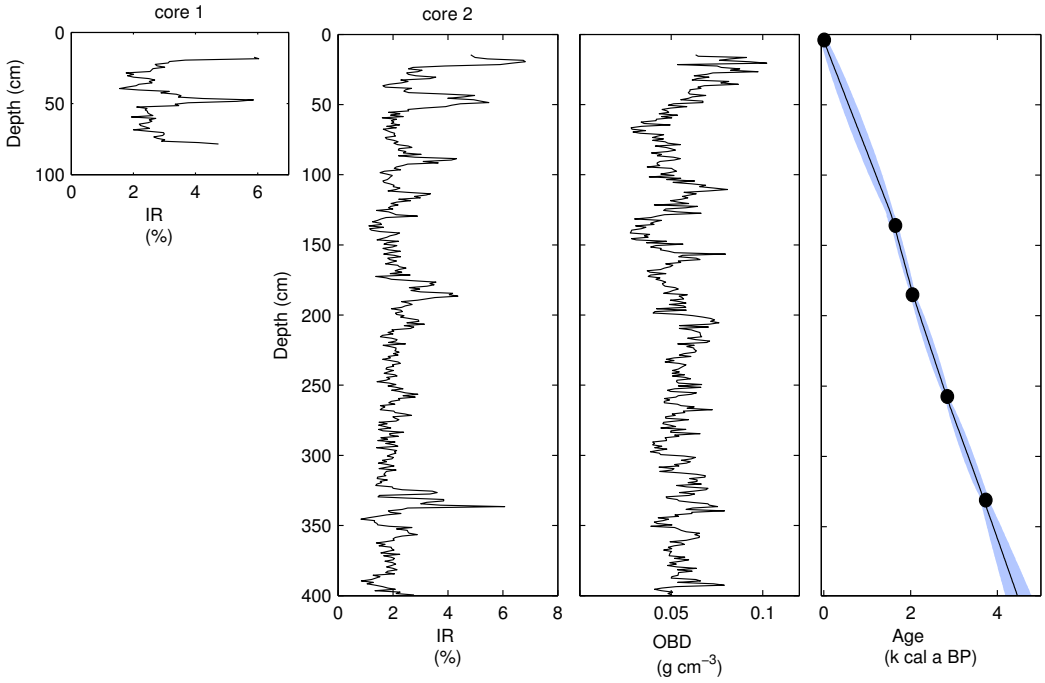

Figure 3:

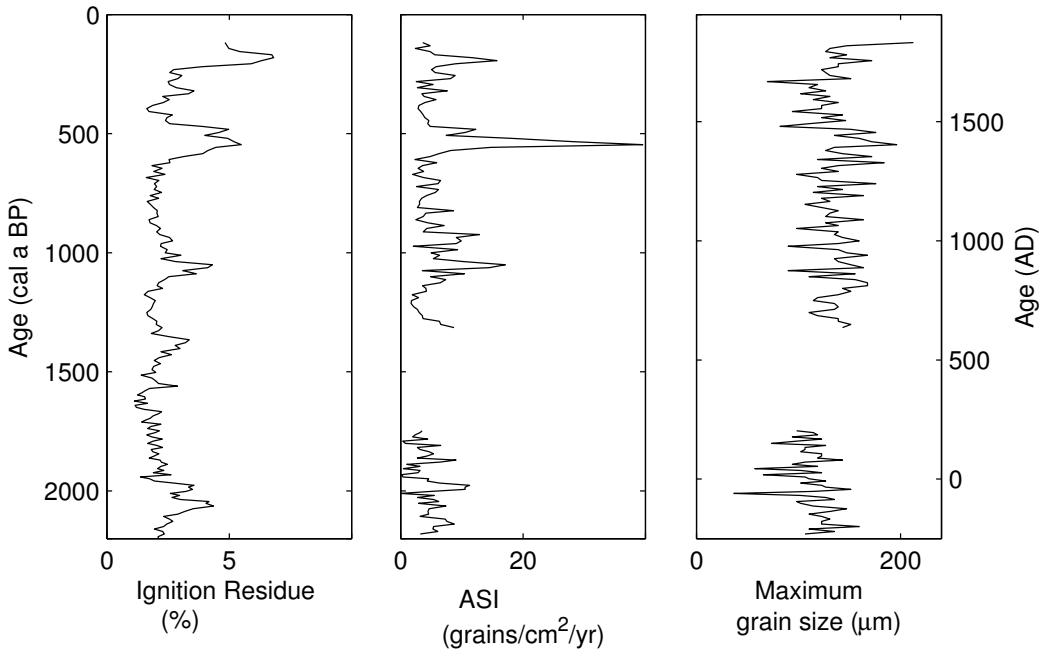

789 Figure 4:

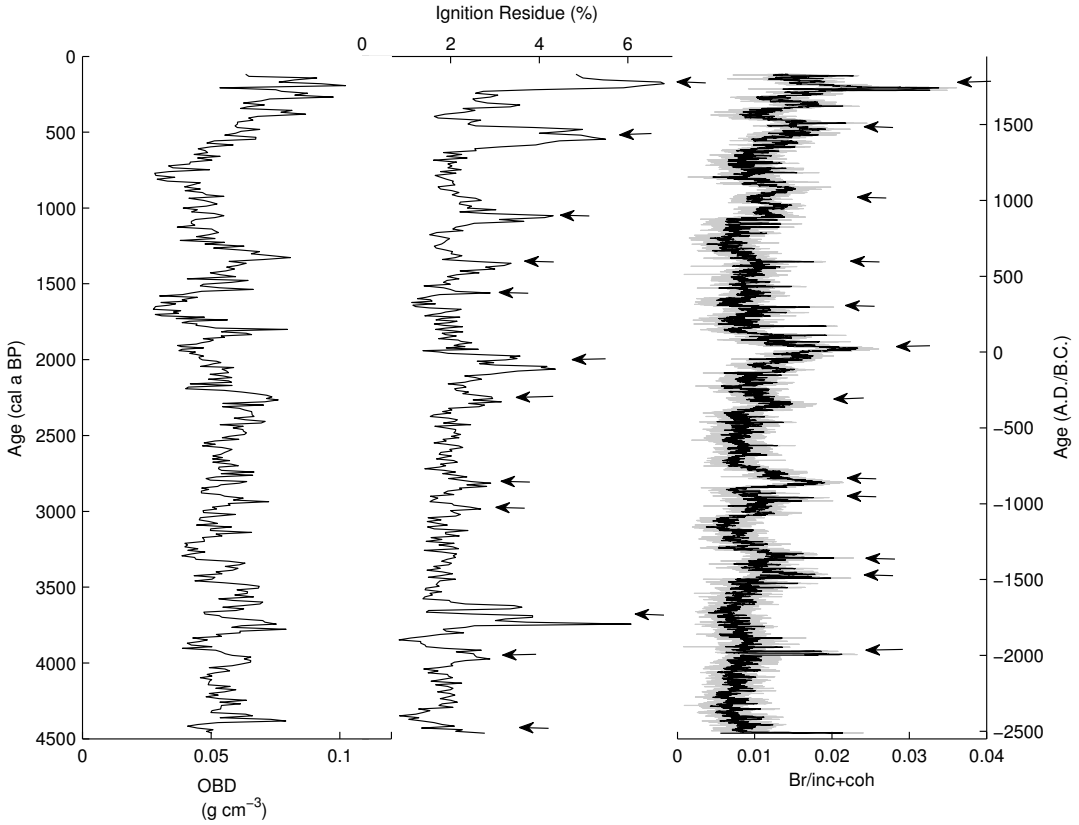

790

791

792

793

794

795

796

797

798

799

800

801

802

803

804

805

806 Figure 5:

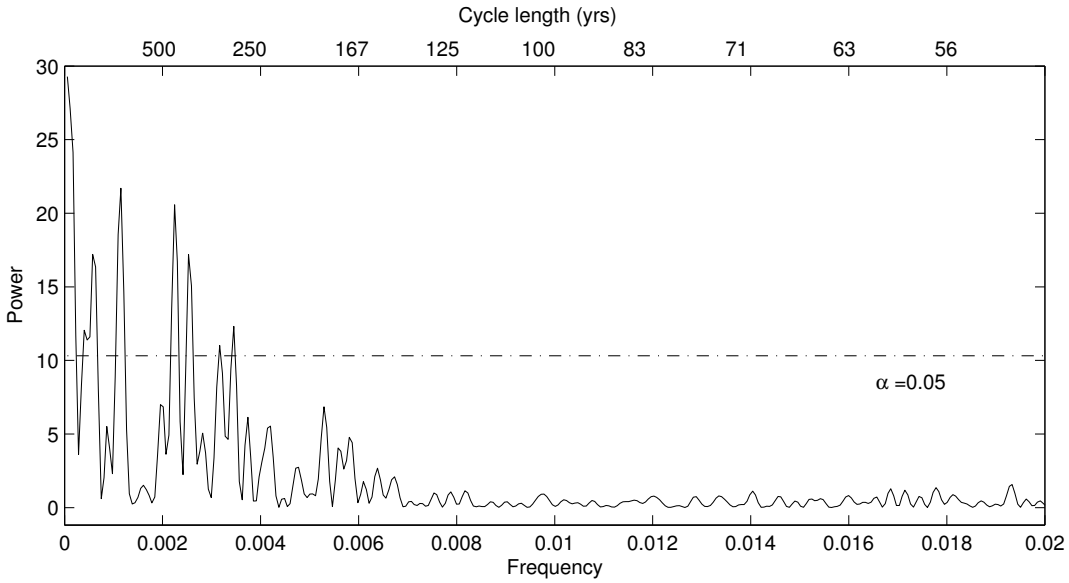

807

808

809 Figure 6:

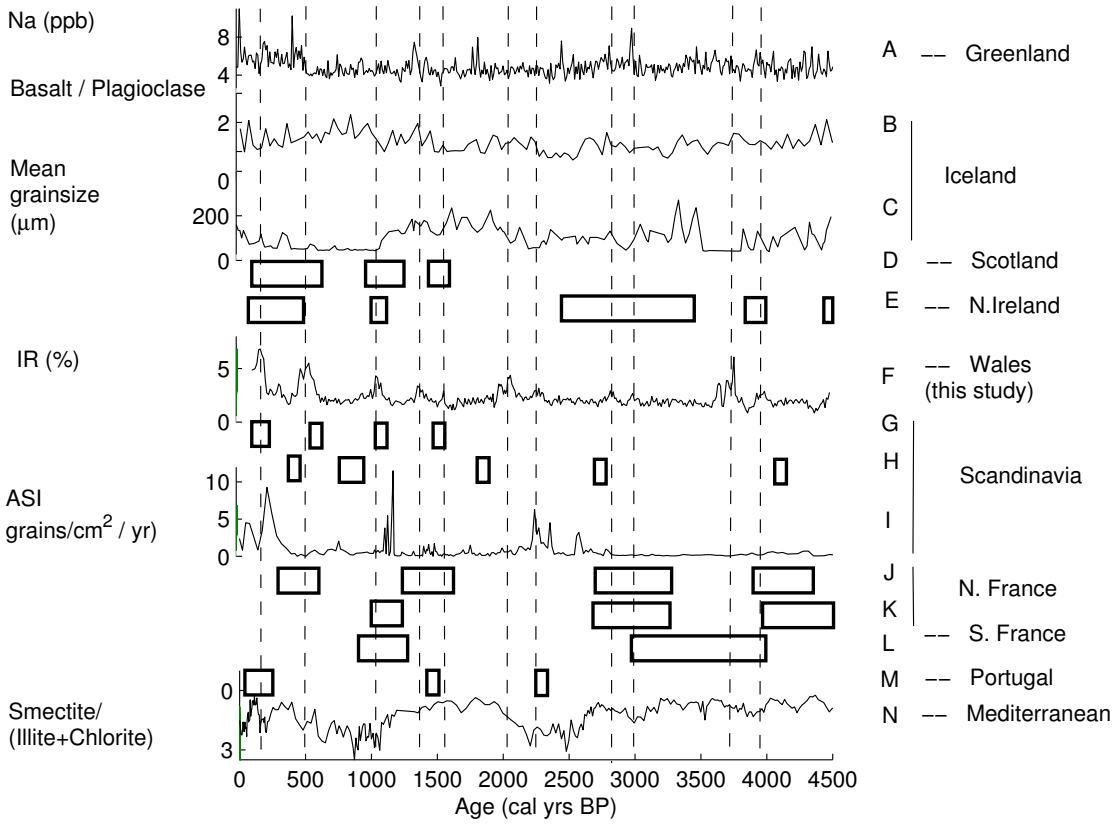

810

811

812 Figure 7:

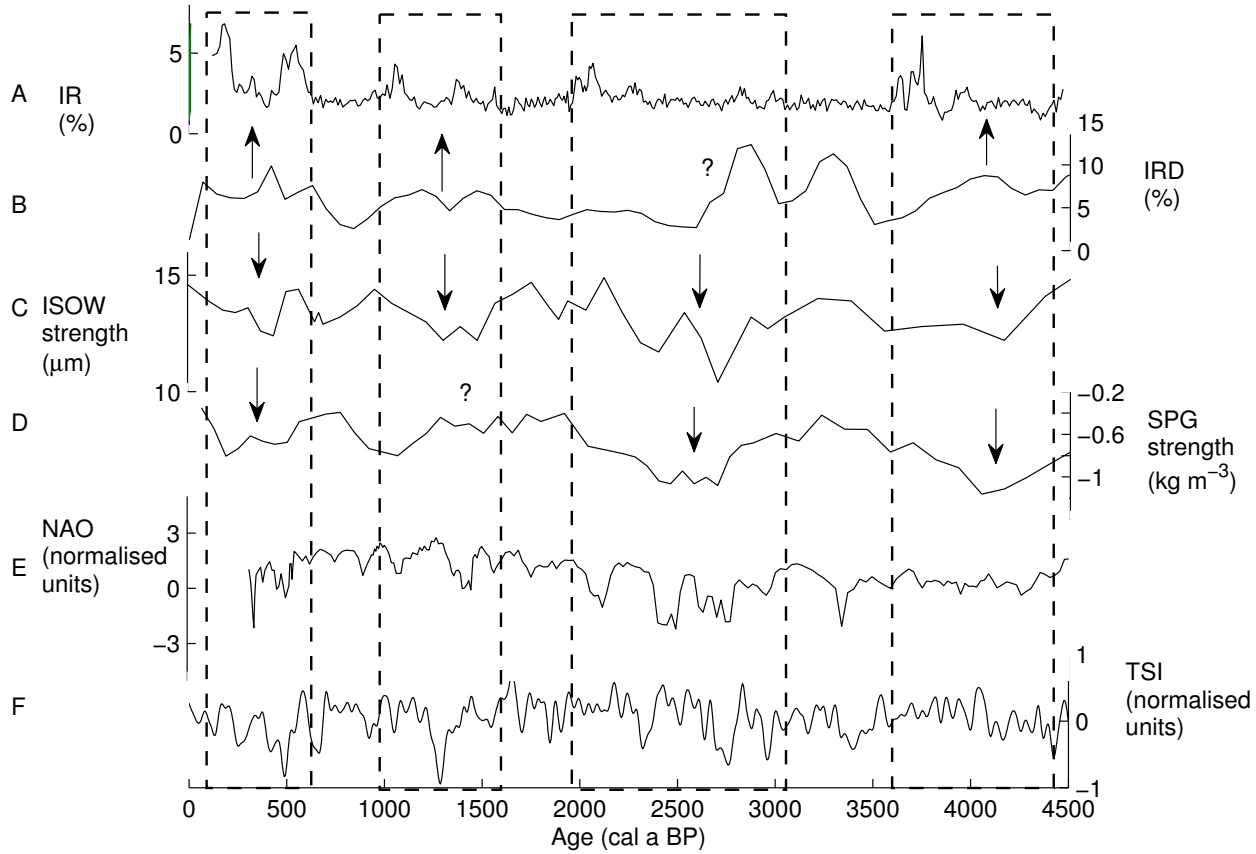

813